

## Electrochemical Aspects of the Synthesis of Iron Particles

Tatjana MALIAR<sup>1</sup>, Julija BOZENKO<sup>1</sup>, Henrikas CESIULIS<sup>1\*</sup>, Igoris PROSYCEVAS<sup>2</sup>

<sup>1</sup> Vilnius University, Department of Physical Chemistry, Naugarduko 24, LT-03225 Vilnius, Lithuania

<sup>2</sup> Institute of Physical Electronics of Kaunas University of Technology, Savanoriu 271, LT-50131 Kaunas, Lithuania

crossref <http://dx.doi.org/10.5755/j01.ms.18.3.2429>

Received 16 May 2011; accepted 19 July 2011

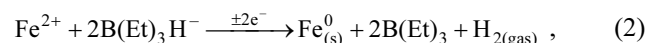
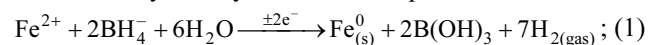
The preparation of Fe-particles by reduction of FeSO<sub>4</sub> with either sodium borohydride or lithium triethylborohydride in water, and reverse micelles in rapeseed and mineral oil phases is described in electrochemical terms. The influence of surfactants on the electrochemical parameters and resulting size of iron particles was studied as well. The resulting size of Fe-particles synthesized in water (with and without surfactants) correlates with the determined values of open circuit potential (OCP): the more negative OCP, the obtained Fe-particles are bigger, because values of OCP correspond to different range of polarization determined for the reduction of Fe<sup>2+</sup>. The sizes of Fe-particles synthesized in water or oil phases without surfactants using LiBEt<sub>3</sub>H are less than using NaBH<sub>4</sub> because of electrochemical factors. By varying oils and surfactants it is possible to obtain opposite results as in water phase: smaller Fe-particles obtained using NaBH<sub>4</sub> than using LiBEt<sub>3</sub>H. It is explained by the simultaneous influence of electrochemical and steric stabilization factors, and the last one becomes dominating in some cases.

*Keywords:* iron particles, synthesis, surfactants, reduction, electrochemistry.

### INTRODUCTION

Magnetic nano-particles are of great interest for researchers from a wide range of disciplines such as magnetic fluids [1], catalysis [2–3], biotechnology and biomedicine [4], magnetic resonance imaging [5–6], data storage [7], environmental remediation [8–9], tribology [10–12], and etc. The four-ball wear and other results of fretting tests indicate that metallic nano-particles are potential additives for lubricating oils, and the tribological performance of lubricating oils can be improved significantly by introduction solid particles such as nickel, iron, CuO, TiO<sub>2</sub>, diamond into oils [13–18].

Frequently colloidal particles of iron-group metals have been prepared via a wet chemical reduction of metal salt by appropriate reduction agent such as sodium hydrazine [19], sodium borohydride [20–21], and lithium triethylborohydride [22]. In aqueous media the obtaining of zero-valent iron by using sodium borohydride and lithium triethylborohydride can be expressed as follows:



where “±2e<sup>-</sup>” means a transfer of two electrons from reducing agent to the Fe<sup>2+</sup>; “Et” is a triethyl group.

In fact, reactions (1) and (2) are electrochemical, because comprise the electron transferring stage.

However, an unavoidable problem associated with small particles is their intrinsic instability over longer periods of time. Such small particles tend to form agglomerates to reduce the energy associated with the high surface area to volume. Moreover, the naked metallic nano-particles are chemically highly active and easily oxidized in air, resulting generally in loss of magnetism, dispersibility, and many other functional properties. For many applications it is

crucial to develop protection strategies to chemically stabilize the naked magnetic nano-particles from oxidation during or after the synthesis. These strategies comprise grafting or coating with organic species, including surfactants or polymers, or coating with an inorganic layer, such as silica or carbon [23], or forming noble shell around magnetic core via covering the surface by more noble metals such as copper [24], silver [25], and gold [26].

The aim of this paper is to study electrochemical aspects of the synthesis of iron particles in water and reverse micelles in oil (mineral and rapeseed) phases, and provide correlations between electrochemical factors and size distribution of obtained particles. The mineral and rapeseed oils as phases had been selected taking into account the further tests of obtained compositions in the tribosystems. Some positive effects of iron particles on wear have been reported by us recently [17–18].

### EXPERIMENTAL

Analytical grade chemicals (Na<sub>2</sub>SO<sub>4</sub>·10H<sub>2</sub>O, NaBH<sub>4</sub>, FeSO<sub>4</sub>·7H<sub>2</sub>O, LiB(C<sub>2</sub>H<sub>5</sub>)<sub>3</sub>H) and distilled water were used to prepare solutions. The pH of the solution was kept at 3.0 ± 0.1 by adding concentrated H<sub>2</sub>SO<sub>4</sub> or NaOH. Rapeseed and mineral (SAE-10) oils were protected from oxidation by adding 0.5 wt % of octadecyl 3, 5-di-(tert)-butyl-4-hydroxyhydrocinnamate (trade mark Irganox 1076). As surfactants monoalkyl polyethylene glycol ethers based on fatty alcohols (trade mark OS-20) and ethylenediamine tetrakis(ethoxylate-block-propoxylate) tetrol, that is X-type surfactant with four linear poly(ethylene oxide) /poly(propylene oxide) di-blocks “arms” radiating from a central amine molecule (trade mark Tetronic 90R4) were used.

Prior the synthesis, surfactants were dissolved either in water, rapeseed or mineral oils at 50 °C–60 °C and cooled down. Then synthesis of iron particles was performed at 20 °C ± 2 °C by mixing components in 10 ml tube and

\*Corresponding author. Tel.: +370-5-2193183; fax.: +370-5-2330987. E-mail address: [henrikas.cesiulis@chf.vu.lt](mailto:henrikas.cesiulis@chf.vu.lt) (H. Cesiulis)

stirring for 2 min.–3 min. using Vortex type mixer. The size distribution of prepared iron particles was measured by Dynamic Light Scattering (DLS) method using Zetasizer Nano S (Malvern Instruments).

The electrochemical investigations were carried out using AUTOLAB 302 system at  $20 \text{ }^\circ\text{C} \pm 2 \text{ }^\circ\text{C}$ . Linear sweep voltammetry were performed using  $0.002 \text{ V}\cdot\text{s}^{-1}$  potential scan rate. Measurements were carried out in a three-electrode cell with saturated silver chloride electrode as the reference, Pt wire netting was served as a counter electrode, and Fe electrode (99.99 % Alfa Aesar) as a working electrode (working area  $0.0079 \text{ cm}^2$ ). All potential values are expressed against the saturated silver chloride electrode. Before each experiment iron electrode was mechanically polished with 2500 grid paper and rinsed in distilled water.

$\text{Fe}^0$  particles for XRD study were synthesized in water phase using reducing agent  $\text{NaBH}_4$ . Coagulated particles were rinsed with water, dried and XRD spectra were recorded. X-ray diffractograms were recorded by Bragg-Brentano layout with a speed of  $0.02 \text{ deg}\cdot\text{s}^{-1}$  using a DRON 3 diffractometer equipped with a Cu anode ( $K_\alpha$ ) and Ni filter. A copper  $\text{Cu } K_\alpha$  radiation source at 30 kV and 30 mA was used for all X-ray diffraction (XRD) measurements. X-ray wavelength was  $\lambda = 1.54056 \text{ \AA}$ .

## RESULTS AND DISCUSSIONS

### Synthesis without surfactants

In all spontaneously occurring reactions the underlying factor (e. g. formation of metallic Fe-particles from salts) is the matter of energy levels as indicated by oxidation-reduction potentials. In order to produce a particle, work is required, that is designated as energy produced by certain chemical reactions. There is a direct ratio between high redox potential and the production of energy, which results in the growth of those particles requiring these factors. In explaining variations in shape and form by different redox potentials, it is interesting to refer to Daniels, Mathews, and Williams (1929) who state that “the more positive value of the redox potential, the more effective is the ion in the higher state of oxidation as an oxidizing agent; and conversely, the more negative oxidation potential, the more powerful is the ion in the lower state of oxidation as a reducing agent.”

The reduction of hydrated  $\text{Fe}^{2+}$  ions to metallic Fe occurs in the presence of reducing agents that cause the shift of the open circuit potential (OCP) of Fe towards more negative potentials (see Figs. 1 and 2). Both  $\text{NaBH}_4$  and  $\text{LiBH}_4$  shift the values of OCP dependently on its concentration: the higher concentration, the shift is bigger in OCP towards negative values. The most negative values of OCP can reach up to  $-1.2 \text{ V}$  in the presence of  $\text{NaBH}_4$  (Fig. 1), and this compound influences on OCP much stronger than  $\text{LiBH}_4$ .

The weighing values of OCP against corresponding positions on the polarization curves (see Fig. 3) show that OCP values match the range in cathodic branch of polarization curve corresponding the maximal rate of  $\text{Fe}^{2+}$  reduction in the presence of  $\text{NaBH}_4$ , whereas OCP in the presence of  $\text{LiBH}_4$  corresponds with inceptive range of  $\text{Fe}^{2+}$  reduction potentials at higher concentrations only.

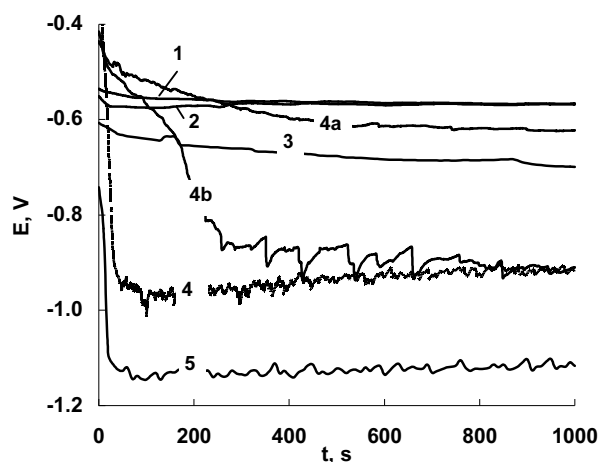


**Fig. 1.** OCP vs. immersion time of Fe-electrode in  $0.5 \text{ M Na}_2\text{SO}_4$  (pH 3.0) with various additions of  $\text{NaBH}_4$  or  $\text{FeSO}_4$ , (in  $\text{mol L}^{-1}$ ): 1 – 0; 2 –  $0.018 \text{ M FeSO}_4$ ; 3 –  $0.0072 \text{ M NaBH}_4$ ; 4 –  $0.036 \text{ M NaBH}_4$  (IV); 4a – IV +  $0.5 \text{ wt}\%$  Tetricon 90R4; 4b – IV +  $0.5 \text{ wt}\%$  OS-20; 5 –  $0.18 \text{ M NaBH}_4$

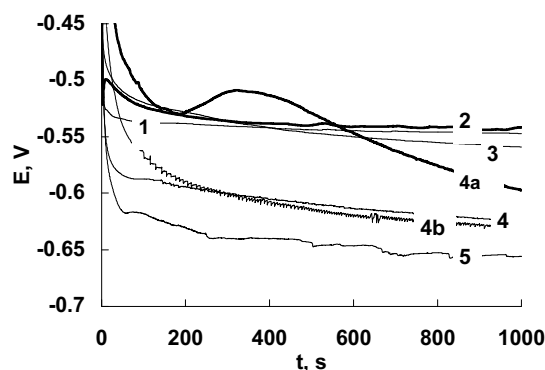


**Fig. 2.** OCP of Fe-electrode in  $0.5 \text{ M Na}_2\text{SO}_4$  (pH 3.0) with various additions of  $\text{LiBH}_4$  or  $\text{FeSO}_4$ , (in  $\text{mol L}^{-1}$ ): 1 – 0; 2 –  $0.018 \text{ M FeSO}_4$ ; 3 –  $0.0072 \text{ M LiBH}_4$ ; 4 –  $0.036 \text{ M LiBH}_4$  (IV); 4a – IV +  $0.5 \text{ wt}\%$  OS-20; 4b – IV +  $0.5 \text{ wt}\%$  Tetricon 90R4; 5 –  $0.09 \text{ M LiBH}_4$

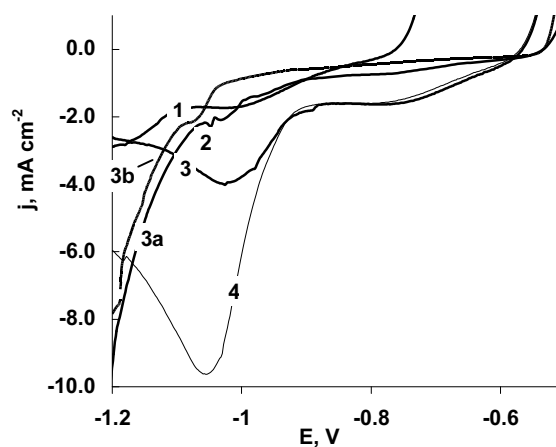


**Fig. 3.** Cathodic polarization curves of Fe-electrode in  $0.5 \text{ M Na}_2\text{SO}_4$  solutions at pH 3 and containing various concentrations of  $\text{FeSO}_4$ : 1 – 0; 2 –  $0.0036 \text{ M}$ ; 3 –  $0.018 \text{ M}$  (III); 3a – III +  $0.5 \text{ wt}\%$  OS-20; 3b – III +  $0.5 \text{ wt}\%$  Tetricon 90R4; 4 –  $0.090 \text{ M}$

Those results in the different rates of appearing Fe-particles in course of reduction by NaBH<sub>4</sub> and LiBEt<sub>3</sub>H in aqueous media, namely, in the presence of NaBH<sub>4</sub> iron particles form almost immediately, whereas in the presence of LiBEt<sub>3</sub>H iron particles appear within 30 min. – 60 min.

The different rates of Fe<sup>2+</sup> reduction to Fe<sup>0</sup> result different sizes of obtained particles using two reducers. If NaBH<sub>4</sub> acts as reducer, the sizes of Fe-particles obtained in water phase and reverse micelles without surfactants are substantially bigger (2–5 times). In all investigated cases obtained Fe-particles are polydispersed and fit the range of sizes rather “meso”. Some characteristic results are presented in Figs. 4 and 5. These data are in line with qualitative peculiarity of colloid chemistry: the higher rate of reaction the bigger particles are formed.

The structure of obtained Fe-powder was studied by the X-ray diffraction method, and XRD pattern is shown in Fig. 6. It consists of one relatively wide peak attributed to the dominating structure {110} of body centred cubic lattice of metallic iron, which is formed in course of synthesis using NaBH<sub>4</sub>. Also some unidentified peaks presence and their intensity is compatible with noise. Usually the structure of Fe particles is concerning as a typical core-shell structure [27]. The core consists primarily of zero-valent or metallic iron while the mixed valent, i. e., Fe(II) and Fe(III) oxide shell is formed as a result of the oxidation of metallic iron. Probably, in this case the thickness of shell is too small in order to form a separate XRD peak representing oxide phase. The mean grain size was estimated from the peak width using the Scherer's equation modified by Warren and Biscece [28]:

$$\beta = \frac{0.94\lambda}{\tau \cos \Theta}; \quad (3)$$

$$\beta^2 = \sqrt{B^2 - b^2}, \quad (4)$$

where  $\beta$  is peak broadening (in radians),  $\lambda$  is the wavelength,  $\tau$  is the grain size,  $\Theta$  is the position of the peak in the XRD pattern,  $b$  is the width of the peak for the crystalline material (MgO acts as standard), and  $B$  is the peak width of the Fe sample.

The calculated value of mean grain size is 26 nm, and this value we consider as a minimal mean size of Fe-particles that can form in water phase at given conditions.

### The effect of surfactants

Evidently, metallic Fe-particles are formed in the presence of reducing agents at OCP. In this case the rate of electroreduction reaction (main reaction is Fe<sup>2+</sup> reduction to Fe<sup>0</sup> or hydrogen evolution reaction in Na<sub>2</sub>SO<sub>4</sub> solution) is equal to the rate of electrooxidation reaction (the main reaction is the oxidation of reducing agent). Every reaction contains multivalent electron transferring stage occurring via complex pathways [29–30]. Therefore, each factor changing the rate of intermediate reactions will influence on the total rate of cathodic and/or anodic reaction resulted in the shift of OCP.

As it is shown in Figs. 1 and 2, the adding of surfactants change values of OCP of Fe-electrode (Tetricon 90R4 with NaBH<sub>4</sub> and OS-20 with LiBEt<sub>3</sub>H), especially the rate of potential shift at the beginning of process. Also, due to

adsorption of surfactant the values of polarization increase (see Fig. 3, curves 3a and 3b). The obtained values of OCP match the inception range of the cathodic branch polarization curve that correlates with decreased rate of particles formation. In the case of particles synthesis, surfactant presenting in the reaction mixture adsorbs and forms a protective shell around Fe-particles that prevents the agglomeration of Fe-particles. Therefore, in the presence of surfactants the size of obtained particles decreases down to nanometer level in water phase (see Figs. 7 and 8).

The data obtained in the presence of surfactant under mentioned conditions also are in line with qualitative peculiarity of colloid chemistry: the higher rates of reaction, the bigger particles are formed.

When Fe-particles are synthesized in the reverse micelles in oil phase, the surfactant molecules can adsorb both on Fe/oil and micelle/oil interfaces. In the last case due to adsorption of surfactant the interfacial tension is lowering, and micelles containing Fe<sup>2+</sup> and reducing agent

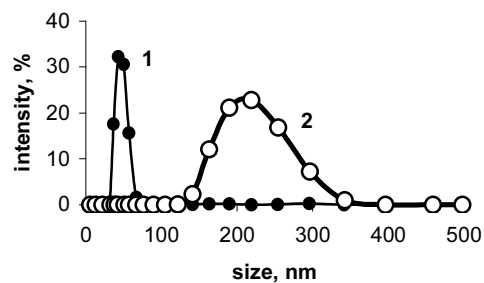


Fig. 4. The size distribution of Fe-particles obtained in aqueous solution in the presence of LiBEt<sub>3</sub>H (1) and NaBH<sub>4</sub> (2). Resulting concentration of Fe-particles is 0.1 wt %

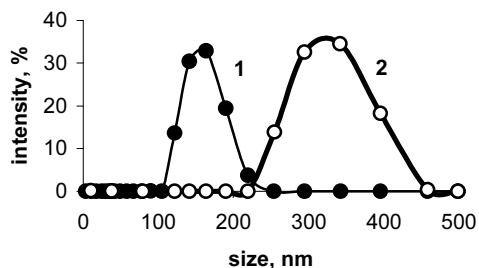


Fig. 5. The size distribution of Fe-particles obtained in the reverse micelles formed in the mineral SAE-10 oil in the presence of LiBEt<sub>3</sub>H (1) and NaBH<sub>4</sub> (2). Resulting concentration of Fe-particles is 0.1 wt %

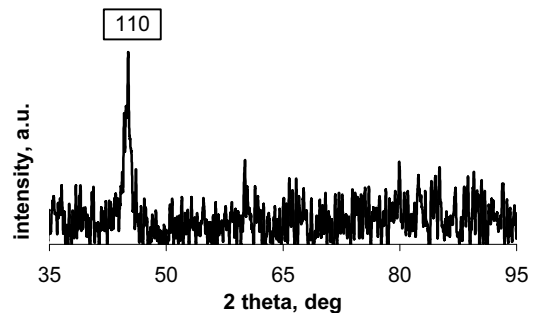
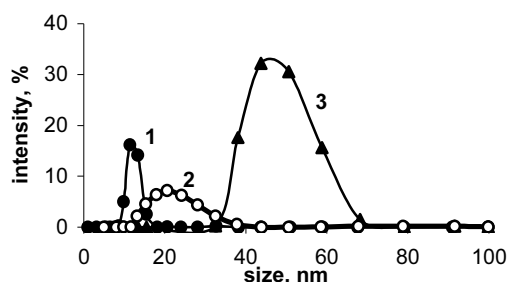
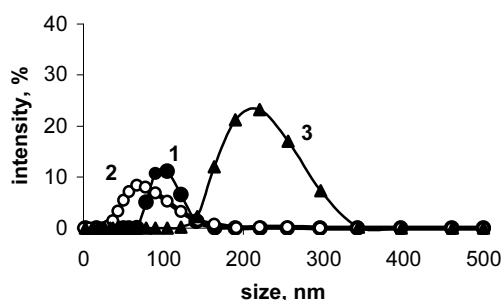


Fig. 6. XRD pattern of Fe powder followed synthesis by the reduction using NaBH<sub>4</sub> as reducing agent in water phase and dried at room temperature



**Fig. 7.** The size distribution of Fe particles obtained in water with adding surfactants: OS-20 (1), Tetrionic 90R4 (2) and without surfactant (3) in the presence of  $\text{LiBEt}_3\text{H}$ . Resulting concentration of Fe particles is 0.1 wt %



**Fig. 8.** The size distribution of Fe particles obtained in water with adding surfactants: OS-20 (1), Tetrionic 90R4 (2) and without surfactant (3) in the presence of  $\text{NaBH}_4$ . Resulting concentration of Fe particles is 0.1 wt %

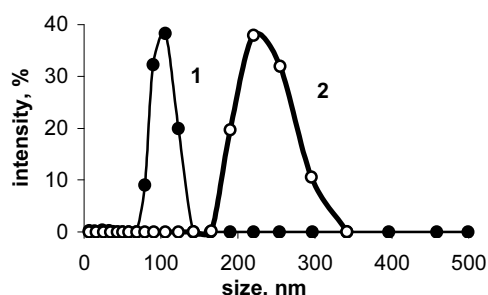


**Fig. 9.** The size distribution of Fe particles obtained in the reverse micelles formed in the rapeseed oil with adding Tetrionic 90R4 as surfactant and in the presence of  $\text{LiBEt}_3\text{H}$  (1) and  $\text{NaBH}_4$  (2). Resulting concentration of Fe particles is 0.1 wt %

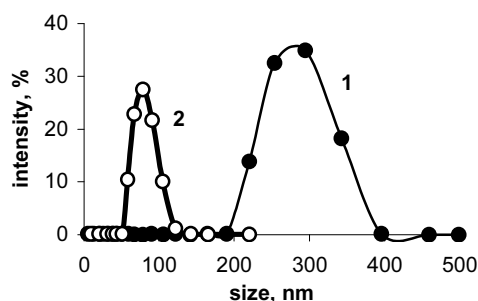


**Fig. 10.** The size distribution of Fe particles obtained in the reverse micelles formed in the mineral SAE-10 oil with adding OS-20 as surfactant and in the presence of  $\text{LiBEt}_3\text{H}$  (1) and  $\text{NaBH}_4$  (2). Resulting concentration of Fe particles is 0.1 wt %

can easier to coalescent during stirring. Moreover, the adsorption of surfactant facilitates the coalescent of released Fe-particles and micelles. Both this factors increase the rate of forming and size of resulting Fe-particles under electrochemical mechanism. On the other hand, adsorbed surfactants form the shells that mechanically prevent the agglomeration of synthesized Fe-particles or prevent the coalescent of micelles, and conditions of synthesis are complicated due to the electrochemical and steric stabilization occurring simultaneously. Therefore, the effect of surfactants on the sizes of Fe-particles becomes unpredictable in advance. This point of view is well illustrated by the data shown in Figs. 9 and 10.

The size of Fe-particles synthesized either in water or oil phase without surfactants using  $\text{LiBEt}_3\text{H}$  are less than using  $\text{NaBH}_4$  because of electrochemical factors (see Figs. 4, 5, 7–9), but by varying oils and surfactants due to dominating steric stabilization mentioned above, it is possible to obtain opposite result: the size of Fe-particles obtained using  $\text{NaBH}_4$  are less than using  $\text{LiBEt}_3\text{H}$  (see Fig. 10).

## CONCLUSIONS

1. The reduction of  $\text{Fe}^{2+}$  ions with  $\text{NaBH}_4$  or  $\text{LiBEt}_3\text{H}$  was used to produce Fe-particles in aqueous media and reverse micelles in oil phases (mineral and rapeseed). The formation of Fe-particle was studied in terms of electrochemistry. The resulting size of Fe-particles synthesized in water (with and without surfactants) correlates with obtained values of open circuit potential (OCP): the more negative OCP, the obtained Fe-particles are bigger, because values of OCP correspond different range of potentials determined for the reduction of  $\text{Fe}^{2+}$ . The sizes of Fe-particles synthesized in water or oil phases without surfactants using  $\text{LiBEt}_3\text{H}$  are less than using  $\text{NaBH}_4$  because of electrochemical factors.

2. By varying oils and surfactants it is possible to obtain opposite results as in water phase: smaller Fe-particles were obtained using  $\text{NaBH}_4$  than using  $\text{LiBEt}_3\text{H}$ . It is explained by the simultaneous influence of electrochemical and steric stabilization factors, and the last one becomes dominating in some cases.

3. Based on XRD pattern, the metallic phase of iron is formed in the course of synthesis using  $\text{NaBH}_4$ . The calculated mean grain size is 26 nm. This value defines a minimal mean size of Fe-particles formed in water at given reaction conditions.

## Acknowledgments

The study was partially supported by Lithuanian Science and Study foundation (grant B-34/2008-09). The authors would like to thank Dr. L. Riauba (AB "Fermentas") for fruitful conversation and assistance of Dynamic Light Scattering methodical analysis of size distribution of Fe-particles.

## REFERENCES

1. Chikazumi, S., Taketomi, S., Ukita, M., Mizukami, M., Miyajima, H., Setogawa, M., Kurihara, Y. Physics of Magnetic Fluids *Journal of Magnetism and Magnetic Materials* 65 (2–3) 1987: pp. 245–251.

2. Lu, A.-H., Schmidt, W., Matoussevitch, N., Bönnemann, H., Spliethoff, B., Tesche, B., Bill, E., Kiefer, W., Schüth, F. Nanoengineering of a Magnetically Separable Hydrogenation Catalyst *Angewandte Chemie* 116 (33) 2004: pp. 4403–4406.
3. Tsang, S. C., Caps, V., Paraskevas, I., Chadwick, D., Thompsett, D. Magnetically Separable, Carbon-supported Nanocatalysts for the Manufacture of Fine Chemicals *Angewandte Chemie* 116 (42) 2004: pp. 5763–5767.
4. Gupta, A. K., Gupta, M. Synthesis And Surface Engineering Of Iron Oxide Nanoparticles For Biomedical Applications *Biomaterials* 26 (18) 2005: pp. 3995–4021. <http://dx.doi.org/10.1016/j.biomaterials.2004.10.012>
5. Mornet, S., Vasseur, S., Grasset, F., Verveka, P., Goglio, G., Demourgues, A., Portier, J., Pollert, E., Duguët, E. Magnetic Nanoparticle Design for Medical Applications *Progress in Solid State Chemistry* 34 (2–4) 2006: pp. 237–247.
6. Li, Z., Wei, L., Gao, M. Y., Lei, H. One-Pot Reaction to Synthesize Biocompatible Magnetite Nanoparticles *Advanced Materials* 17 (8) 2005: pp. 1001–1005.
7. Hyeon, T. Chemical Synthesis of Magnetic Nanoparticles *Chemical Communications* 8 2003: pp. 927–934.
8. Li, X.-Q., Elliott, D. W., Zhang, W.-X. Zero-valent Iron Nanoparticles for Abatement of Environmental Pollutants: Materials and Engineering Aspects *Critical Reviews in Solid State and Materials Sciences* 31 (4) 2006: pp. 111–122. <http://dx.doi.org/10.1080/10408430601057611>
9. Guha, S., Bhargava, P. Removal of Chromium from Synthetic Plating Waste by Zero-valent Iron and Sulfate-reducing Bacteria *Water Environment Research* 77 (4) 2005: pp. 411–416.
10. Belyaev, S., Jankauskas, V. Lubricating Effect of Metal Nanoparticles in Oil on Medium Carbon Steel *Proceedings of the International Conference BALTRIB'2007* 2007: pp. 84–88.
11. Melnikov, V. G. Selective Transfer in Friction of Metal-glass Materials in Alkali Solutions and Control of These Processes *Wear Resistance Effect and Tribotechnology* 2 1992: pp. 20–26 (in Russian).
12. Melnikov, V. G. Development and Application of Antifriction Powders with Active Neutral Additives *Wear Resistance Effect and Tribotechnology* (3–4) 1994: pp. 19–24 (in Russian).
13. Qiu, S., Zhou, Zh., Dong, J., Chen, G. Preparation of Ni Nanoparticles and Evaluation of Their Tribological Performance as Potential Additives in Oils *Journal of Tribology* 123 (3) 2001: pp. 441–444.
14. Kotnarowski, A. Tribological Properties of Oils Modified with the Addition of Metals Nanoparticles. In *Mechanotronic Systems and Materials*. Book Series: *Solid State Phenomena* 113 2006: pp. 393–398.
15. United States Patent 6945699 B2. Bearing Having Anodic Nanoparticle Lubricant, 2005.
16. Wu, Y. Y., Tsui, W. C., Liu, T. C. Experimental Analysis of Tribological Properties of Lubricating Oils with Nanoparticle Additives *Wear* 262 (7–8) 2007: pp. 819–825.
17. Padgurskas, J., Rukuiža, R., Kreivaitis, R., Kupcinskas, A., Jankauskas, V., Cesiulis, H., Maliar, T., Prosycevas, I. Tribological Properties of Mineral Oils Modified with Metallic Nano-particles *Proceedings of the International Conference BALTRIB'2009* 2009: pp.69–76.
18. Maliar, T., Achanta, S., Cesiulis, H., Drees, D. Effect of Iron Micro-/nano-particle Additives on Tribological Behavior of Lubricating Oils *Proceedings of the International Conference BALTRIB'2009* 2009: pp.77–82.
19. Wu, S.-H., Chen, D.-H. Synthesis and Characterization of Nickel Nanoparticles by Hydrazine Reduction in Ethylene Glycol *Journal of Colloid and Interface Science* 259 (2) 2003: pp. 282–286.
20. Fan, M., Yuan, P., Zhu, J., Chen, T., Yuan, A., He, H., Chen, K., Liu, D. Core-shell Structured Iron Nanoparticles Well Dispersed on Montmorillonite *Journal of Magnetism and Magnetic Materials* 321 (20) 2009: pp. 3515–3519.
21. Kuo, C. H., Ehrman, Sh. H. Synthesis of Iron Nanoparticles via Chemical Reduction with Palladium Ion Seeds *Langmuir* 23 (3) 2007: pp. 1419–1426.
22. Guo, Z., Henry, L. L., Palshin, V., Podlaha, E. J. Synthesis of Poly(methyl methacrylate) Stabilized Colloidal Zero-valence Metallic Nanoparticles *Journal of Materials Chemistry* 16 (18) 2006: pp. 1772–1777. <http://dx.doi.org/10.1039/b515565g>
23. Lu, A.-H., Salabas, E. L., Schüth, F. Magnetic Nanoparticles: Synthesis, Protection, Functionalization, and Application *Angewandte Chemie International Edition* 46 (8) 2007: pp. 1222–1244.
24. Guo, Z., Kumar, C., Henry, L. L., Doomes, E. E., Hormes, J., Podlaha, E. J. Displacement Synthesis of Cu Shells Surrounding Co Nanoparticles *Journal of the Electrochemical Society* 152 (1) 2005: pp. D1–D5.
25. Bala, T., Arumugam, S. K., Pasricha, R., Prasad, B. L. V., Sastry, M. Foam-based Synthesis of Cobalt Nanoparticles and Their Subsequent Conversion to Co<sub>core</sub>Ag<sub>shell</sub> Nanoparticles by a Simple Transmetalation Reaction *Journal of Materials Chemistry* 14 (6) 2004: pp. 1057–1061.
26. Zhou, W. L., Carpenter, E. E., Lin, J., Kumbhar, A., Sims, J., O'Connor, C. J. Nanostructures of Gold Coated Iron Core-shell Nanoparticles and the Nanobands Assembled under Magnetic Field *The European Physical Journal D* 16 (1) 2001: pp. 289–292. <http://dx.doi.org/10.1007/s100530170112>
27. Li Xiao-qin, Elliott, D. W., Wei-xian Zhang. Zero-Valent Iron Nanoparticles for Abatement of Environmental Pollutants: Materials and Engineering Aspects *Critical Reviews in Solid State and Materials Sciences* 31 (41) 2006: pp. 111–122.
28. Warren, B. E., Bisce, J. The Structure of Silica Glass by X-ray Diffraction Studies *Journal of the American Ceramic Society* 21 (2) 1938: pp. 49–54.
29. Finkelstein, D. A., Mota, N. D., Cohen, J. L., Abrun, H. D. Rotating Disc Electrode (RDE) Investigation of BH<sup>-</sup> and BH<sub>3</sub>OH<sup>-</sup> Electro-oxidation at Pt and Au: Implications for BH<sub>4</sub><sup>-</sup> Fuel Cells *Journal of Physical Chemistry C* 113 (46) 2009: pp. 19700–19712. <http://dx.doi.org/10.1021/jp900933c>
30. Grande, W. C., Talbot, J. B. Electrodeposition of Thin Films of Nickel-iron, II Modelling *Journal of the Electrochemical Society* 140 (3) 1993: pp. 675–681. <http://dx.doi.org/10.1149/1.2056141>

Presented at the 20th International Baltic Conference "Materials Engineering 2011" (Kaunas, Lithuania, October 27–28, 2011)